PHILOSOPHICAL TRANSACTIONS OF THE ROYAL SOCIETY A MATHEMATICAL, PHYSICAL & ENGINEERING SCIENCES

Neutron-deficient nuclei studied with stable and radioactive beams

W. Gelletly and P. J. Woods

Phil. Trans. R. Soc. Lond. A 1998 **356**, 2033-2062
doi: 10.1098/rsta.1998.0262

THE ROYAL SOCIETY

Neutron-deficient nuclei studied with stable and radioactive beams

By W. Gelletly[1] and P. J. Woods[2]

[1]*School of Physical Sciences, University of Surrey, Guildford GU2 5XH, UK*
[2]*Department of Physics and Astronomy, University of Edinburgh, Edinburgh EH9 3JZ, UK*

Neutron-deficient nuclei close to the proton drip-line have been studied intensively in recent years. Measurements of ground-state proton emitters have mapped out the limits of nuclear stability above ^{100}Sn. Such experiments have allowed us to learn about the single-particle shell structure far from stability. Studies of γ-rays from $N = Z$ nuclei produced in fusion–evaporation reactions have revealed that their properties vary rapidly with small changes in Z, N and A because of large oblate and prolate shell gaps at large deformation. Studies of these nuclei also reveal information about isospin mixing as a function of mass and potentially yield information about n–p pairing.

The astrophysical rp-process pathway lies close to the $N = Z$ line. Studies of fragmentation reactions have allowed us to determine a lot of the information needed to analyse the rp-process in detail. All of this information is limited, however, by the constraint of using stable beams and targets. With beams of radioactive nuclei, classical spectroscopic techniques such as Coulomb excitation and particle transfer studies will allow us to map out level properties in detail in nuclei far from stability. Studies of fusion–evaporation reactions with beams of radioactive ions by using new, more sensitive detection techniques will allow us to study nuclei up to and beyond the drip-line in nuclei above ^{100}Sn. At the same time such studies will allow us much greater access to the lighter $N = Z$ nuclei.

Keywords: exotic nuclei; proton drip-line; radioactive beams

1. Introduction

Among the major themes in nuclear structure physics over the past 15 years or so has been the steady advance in our knowledge of nuclear properties under extreme conditions. As with all physical systems, the properties of the nucleus can be understood in terms of the variation of a small number of key parameters. A simple analogy would be that unless we were able to vary the temperature of water we would never know that it could become a solid or a vapour. Figure 1 shows in schematic form (Richter 1993) the landscape created by some of the key parameters for the nucleus: energy E (or temperature), angular momentum J, and the ratio of neutrons to protons (N/Z).

We have been exploring how nuclear properties vary with all of these parameters. For example, there has been a huge advance in our knowledge of how nuclei behave under the stress of high rotational velocity. Most, but not all, of this advance in our knowledge has come from studies of the high-multiplicity cascades of γ-rays emitted in the decay of the compound nuclei formed in fusion–evaporation reactions

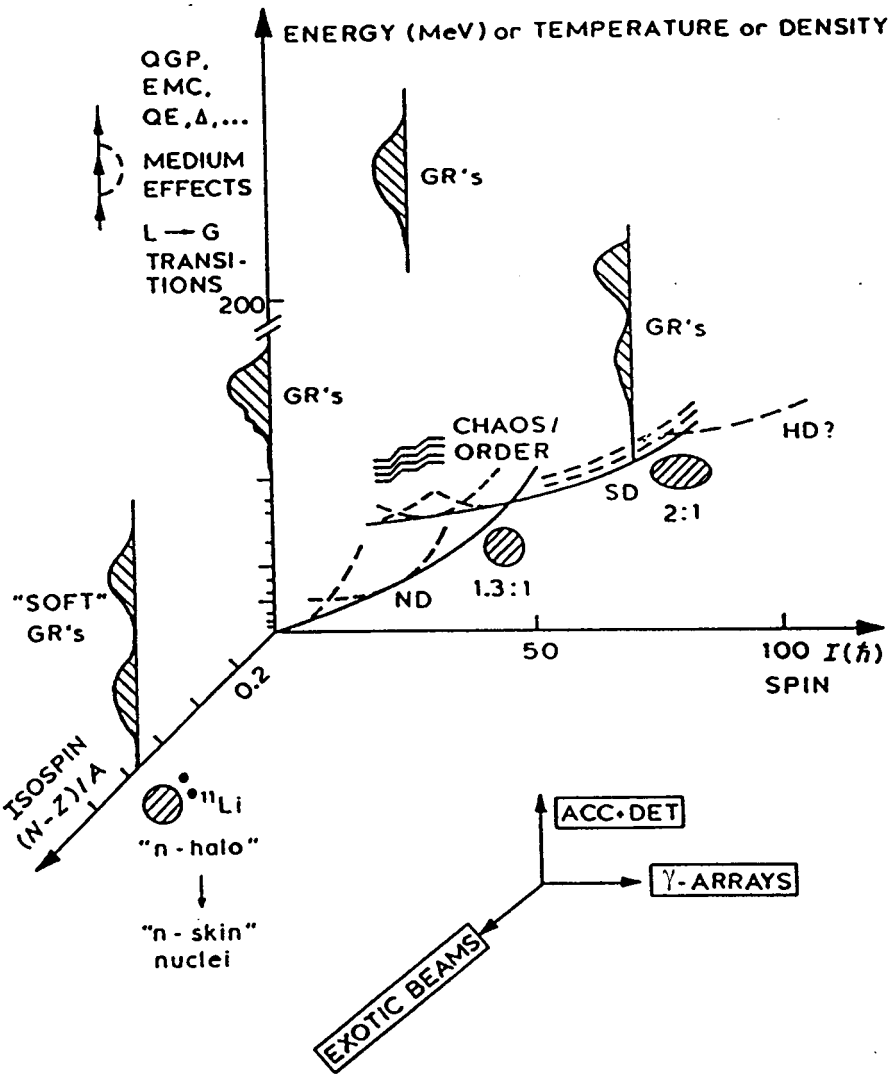

Figure 1. Parameters of importance in studying nuclear structure.

(see below). These studies have driven and in turn been stimulated by the rapid development of arrays of Compton-suppressed Ge detectors (Beausang & Simpson 1996). Such reactions have also been one of the main vehicles for creating neutron-deficient nuclei, the subject of this article.

Figure 2 shows one version of the chart of the nuclides or Segré chart. It shows the stable nuclei, the black squares, as a function of proton (Z) and neutron (N) number. Each square represents a nucleus with a particular combination of N and Z. Estimates of the locations of the proton and neutron drip-lines, the locus of points joining those nuclei where the last proton or neutron is no longer bound, are shown as continuous lines. The blank spaces between the drip-lines are filled by unstable nuclear species. In this article we will be concerned with the properties of the most neutron-deficient nuclei which form the proton drip-line or lie close to it.

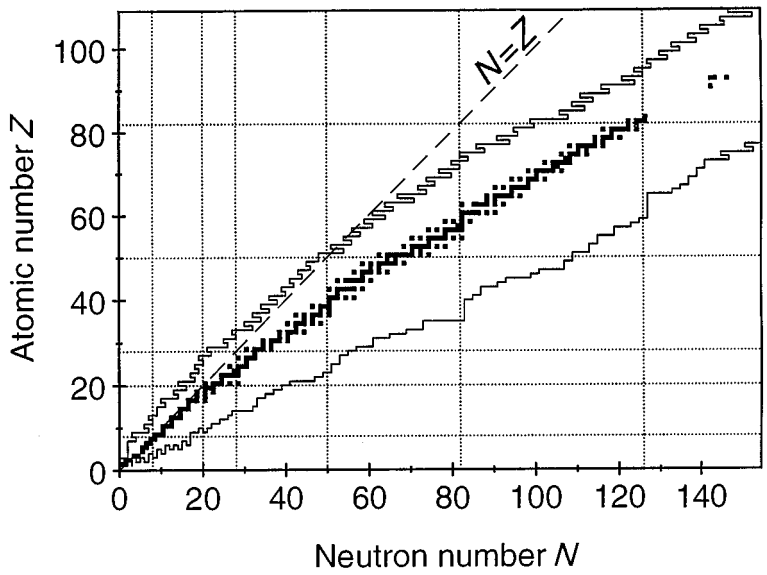

Figure 2. The figure shows a version of the chart of the nuclides. The stable nuclear species, shown as black squares, are plotted as a function of atomic number (Z) and neutron number (N). Estimates of the proton and neutron drip-lines are shown as continuous lines. Unstable nuclear species fill the remaining space between the drip-lines.

In §§ 2 and 3 we will outline the interest in neutron-deficient nuclei, how they have been studied to date with stable beams, and a summary of our present knowledge of such nuclei. In § 4 we will discuss how the availability of improved beams of radioactive nuclei promises to alter this situation.

2. Nuclei on or near the $N = Z$ line

(*a*) *Introduction*

Nuclei with equal numbers of neutrons and protons are of particular interest for several reasons. Up to ^{100}Sn the neutrons and protons fill the same shells. As a result, the nuclear shape depends initially on Z, N and angular momentum; a small change in Z or N can result in quite dramatic changes in nuclear deformation (Gelletly 1995). In some cases it also leads to the coexistence of prolate, oblate and spherical shapes (Nazarewicz *et al*. 1985), i.e. states in the same nucleus of quite different shape but similar excitation energy. Nuclei with $N = Z$ are also of special interest because of what they reveal about a variety of symmetries. It is well established that the interactions between nucleons are charge independent. Consequently, the properties of the $N = Z$ nuclei provide us with a laboratory for studying such symmetries and their violation. It is in these nuclei that we might also expect to observe the effect of n–p pairing.

It turns out, however, that such nuclei are difficult to study since the disruptive effect of the Coulomb interaction causes stable isotopes to have an increasing excess of neutrons as Z increases. Eventually, $N = Z$ nuclei cease to exist when the proton drip-line is crossed just above the doubly magic nucleus ^{100}Sn, as can be seen in figure 2. In essence most of our knowledge of $N = Z$ nuclei is derived from stud-

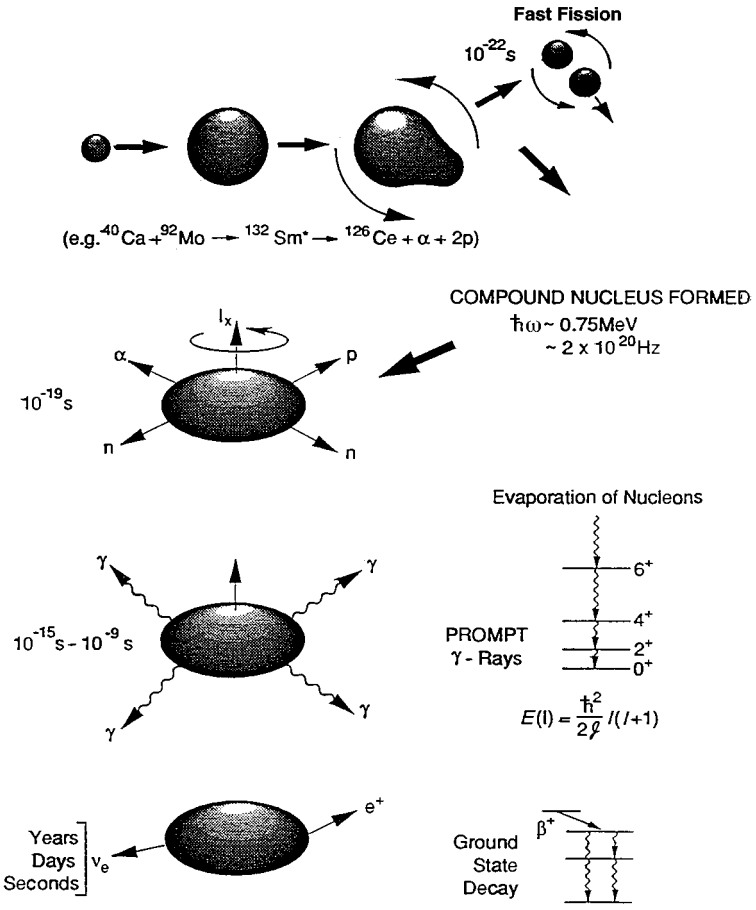

Figure 3. A schematic version of how fusion–evaporation reactions proceed (see text).

ies of fusion–evaporation reactions and β-decay. Figure 3 shows schematically our understanding of how fusion–evaporation reactions proceed. When two heavy nuclei or ions come together they may scatter from one another or the system may fission rapidly. However, close to the Coulomb barrier the cross-section for fusion of the two nuclei is large, typically of the order of a barn. The compound nucleus is hot (at high excitation energy), and rotates with high angular momentum (typically 50–60 $\hbar$). On a typical nuclear time-scale, 10^{-22} s is the time for a nucleon to cross the nucleus. This compound nucleus lives for a relatively long time, *ca.* 10^{-17} s. In this state we can see the nucleus as a hot, rotating liquid drop and like any such droplet it will cool down by evaporating particles. It emits protons, neutrons and α-particles. This will reduce the temperature but leave quite a lot of energy tied up in rotation. Now the cooling process can only continue with the emission of a long cascade of γ-rays leading eventually through the ground-state rotational band to the ground state itself. This long cascade of γ-rays carries a lot of information about the nuclear structure of the product nucleus. To date it has been the main source of information about all but the lightest $N = Z$ nuclei.

With beams and targets of stable nuclei the compound nucleus will inevitably be

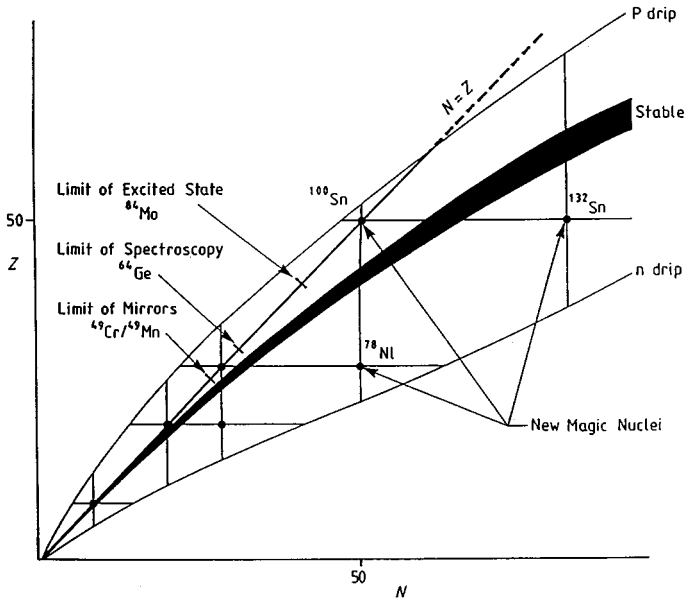

Figure 4. A version of the chart of the nuclides showing the present extent of our knowledge of $N = Z$ nuclei as gleaned from γ-ray spectroscopy.

neutron-deficient (see figure 2) since the N/Z ratio for stable nuclei steadily increases with A. Near the line of nuclear stability neutron emission from the compound nucleus is heavily favoured, and such reactions will lead to more neutron-deficient nuclei. However, the relative probabilities of emission of neutrons, protons and α-particles depend critically on the binding energies of these particles. Accordingly, as we try to form more and more neutron-deficient nuclei, which requires neutron emission, the probability falls rapidly. We will see examples below.

The nuclei at or near the $N = Z$ line have also been studied in β-decay, with the β-decaying nuclei being produced in the spallation of high-energy protons or in (HI,xn) reactions. Beta-decay studies are limited by the constraints of selection rules to states of angular momentum close to that of the parent state, but they yield invaluable information inter alia on the strength of the weak interaction (Hardy *et al*. 1990), isospin mixing (Nagarajan *et al*. 1996) as well as on nuclear structure (Oinonen *et al*. 1998; Honkanen *et al*. 1996).

More recently, it has become possible to form weak beams of these nuclei with $N \sim Z$ in the fragmentation of high-energy, heavy ions. These beams can be used to induce secondary reactions or can be studied themselves. Several experiments of this kind have been used to determine the existence of exotic nuclear species in the region between the $N = Z$ line and the proton drip-line. In the same experiments isomeric states have been identified in some nuclei and the β-decay half-lives of others have been measured.

(*b*) *Gamma-ray spectroscopy of* $N = Z$ *nuclei*

We have asserted above that the properties of $N = Z$ nuclei are of special interest. It is of importance to know how much we have learned about them so far. The

situation is summarized in figure 4, where we see a schematic version of the nuclear chart.

The heaviest, even–even nucleus identified (Gelletly *et al*. 1991) by detecting γ-ray transitions emitted in a fusion–evaporation reaction is ^{84}Mo. In this case only a single γ-ray was observed from the reaction, which was assigned as the 2_1^+–0_1^+ transition in the ground-state band. More recently, γ-rays from the decay of an isomeric state in odd–odd ^{86}Tc, populated in fragmentation, have been observed (Regan *et al*. 1997).

In both these cases the observation of only a few γ-rays provides very limited information. Real spectroscopy requires rather more. In these terms the limit of spectroscopy is ^{64}Ge in the case of even–even nuclei (Ennis *et al*. 1991). However, a level scheme has now been obtained for ^{72}Kr (De Angelis *et al*. 1998), and this is shown in figure 5. The result of significance here is that the energies of the first few states suggest oblate-prolate shape coexistence with the ground state being oblate. The results of a whole series of experiments on the even–even $N = Z$ nuclei are summarized in figure 6. Here we see the 2_1^+ level energies plotted as a function of mass. The quadrupole deformation ε_2 can be derived from the energies by using the empirical relationship,

$$B(E2; 2^+\text{–}0^+) = \frac{(94 \pm 17)Z^2}{A^2 E(2^+)} Wu,$$

from Raman *et al*. (1991), which is based on the earlier work of Grodzins (1966). The lower part of figure 6 shows ε_2 derived from the empirical relationship of Grodzins (1966). The deformation reaches a peak for ^{76}Sr/^{80}Zr, which are among the most deformed nuclei known in their ground states. Confirmation of these results comes from laser resonance fluorescence studies (Lievens *et al*. 1992) of the properties of ^{77}Sr in its ground state. They show $J^\pi = \frac{5}{2}+$, $\mu = 0.348\,\mu_\mathrm{m}$ and $Q = +1.40(11)$ b for this state. This is consistent with the 39th and last neutron in ^{77}Sr being in the [4 2 2] 5/2+ Nilsson orbital with $\beta_2 = +0.40$.

Returning to figure 4, we note that the mirror nuclei ^{49}Mn and ^{49}Cr are the heaviest pair of such nuclei which have been studied. Mirror nuclei have been well studied in the form of isobaric multiplets in light nuclei, but little is known about their behaviour as a function of angular momentum. The ^{49}Mn–^{49}Cr pair was first studied (Cameron *et al*. 1990, 1991) at Daresbury Laboratory and more recently (O'Leary *et al*. 1997) at Riso. The resulting level schemes are shown in figure 7. The striking similarity in the two level schemes comes as no surprise given our belief in the charge independence of nuclear forces. Initially, however, it came as a surprise that the level structures were collective in nature given the small number of valence particles involved. A plot of J versus $\hbar\omega$ derived from the level energies reveals that there is an alignment of two $f_{7/2}$ particles at $J \sim 17/2$. This is consistent with the results of cranked shell-model calculations. Figure 8 shows the difference in level energies for ^{49}Mn and ^{49}Cr plotted as a function of spin. It is striking that this Coulomb energy difference rises rapidly just at the point where the particle alignment occurs. Can we explain this?

In crude terms the alignment in ^{49}Mn must be due to the protons since the neutron orbitals are blocked. Similarly the alignment in ^{49}Cr must be due to the neutrons. When the alignment occurs the two particles move apart, thus decreasing the Coulomb energy in the case of ^{49}Mn and leaving it unaffected in first order in ^{49}Cr. The result is an increase in the Coulomb energy difference just as seen in figure 8.

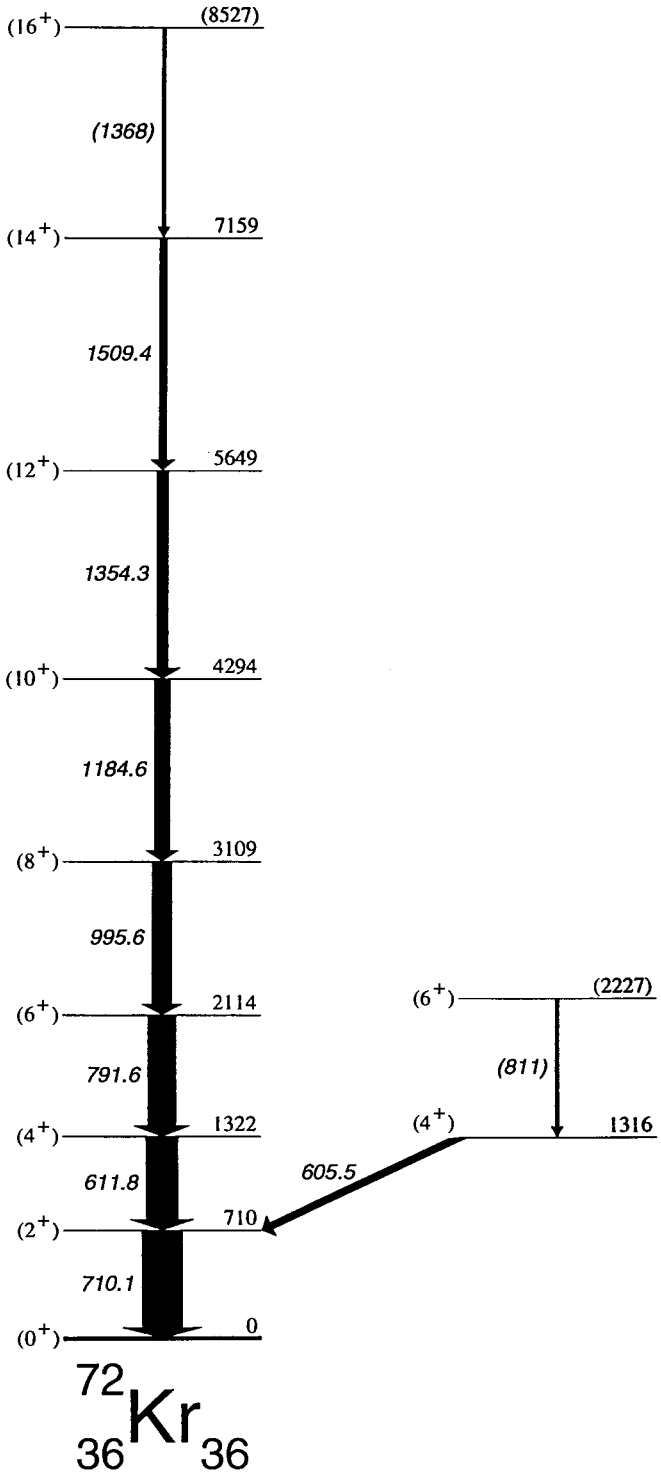

Figure 5. The level scheme of the even–even, $N = Z$ nucleus ^{72}Kr (De Angelis *et al*. 1998).

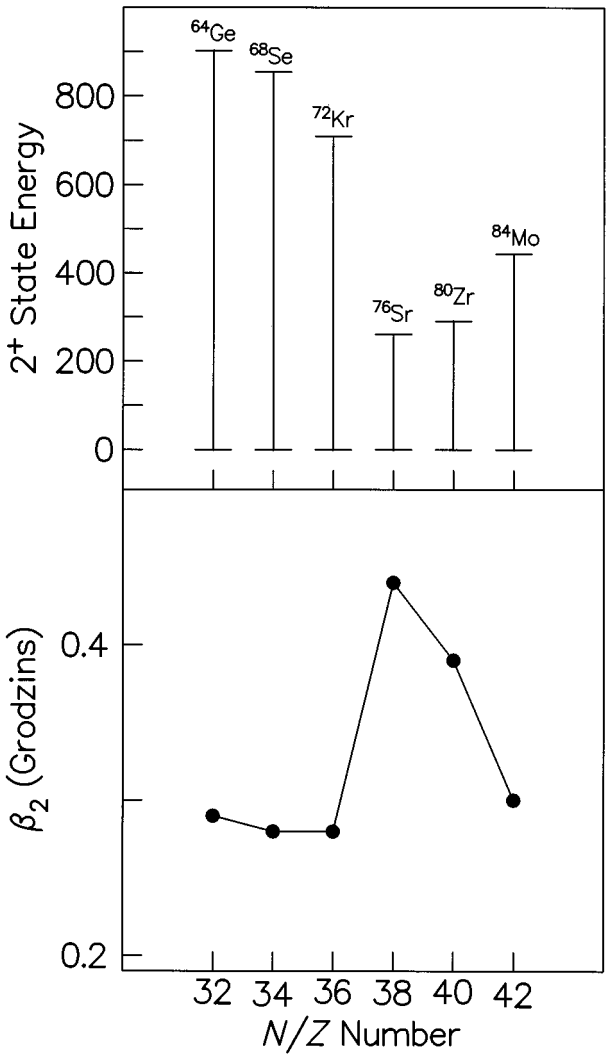

Figure 6. The upper part of the figure shows the excitation energies of the first 2^+ states in the $N = Z$, even–even nuclei up to ^{84}Mo. The lower half shows corresponding values of the quadrupole deformation β_2 derived from the semi-empirical relationship of Grodzins (1966).

Eventually, when the alignment is completed this difference returns to zero. Whether this 'handwaving' explanation is correct, or whether it is due to non-collective effects in a limited single-particle space, requires us to study further cases. Apart from a few nuclei near the $A = 49$ pair the most promising cases are the heavier mirror pairs such as ^{75}Rb–^{75}Sr, where the nuclei are more deformed. To date they have not been studied because the cross-sections of the reactions leading to them are too small.

The steady increase in the Coulomb force with increasing Z leads to increased isospin mixing (Nagarajan *et al*. 1996). For example, Hamamoto & Sagawa (1993) suggested that it will increase to *ca*. 5% in ^{80}Zr. This can be studied in β-decay as well as in the level schemes derived from fusion–evaporation reactions. In β-decay it manifests itself in the log ft values for superallowed Fermi decays. The effect can also

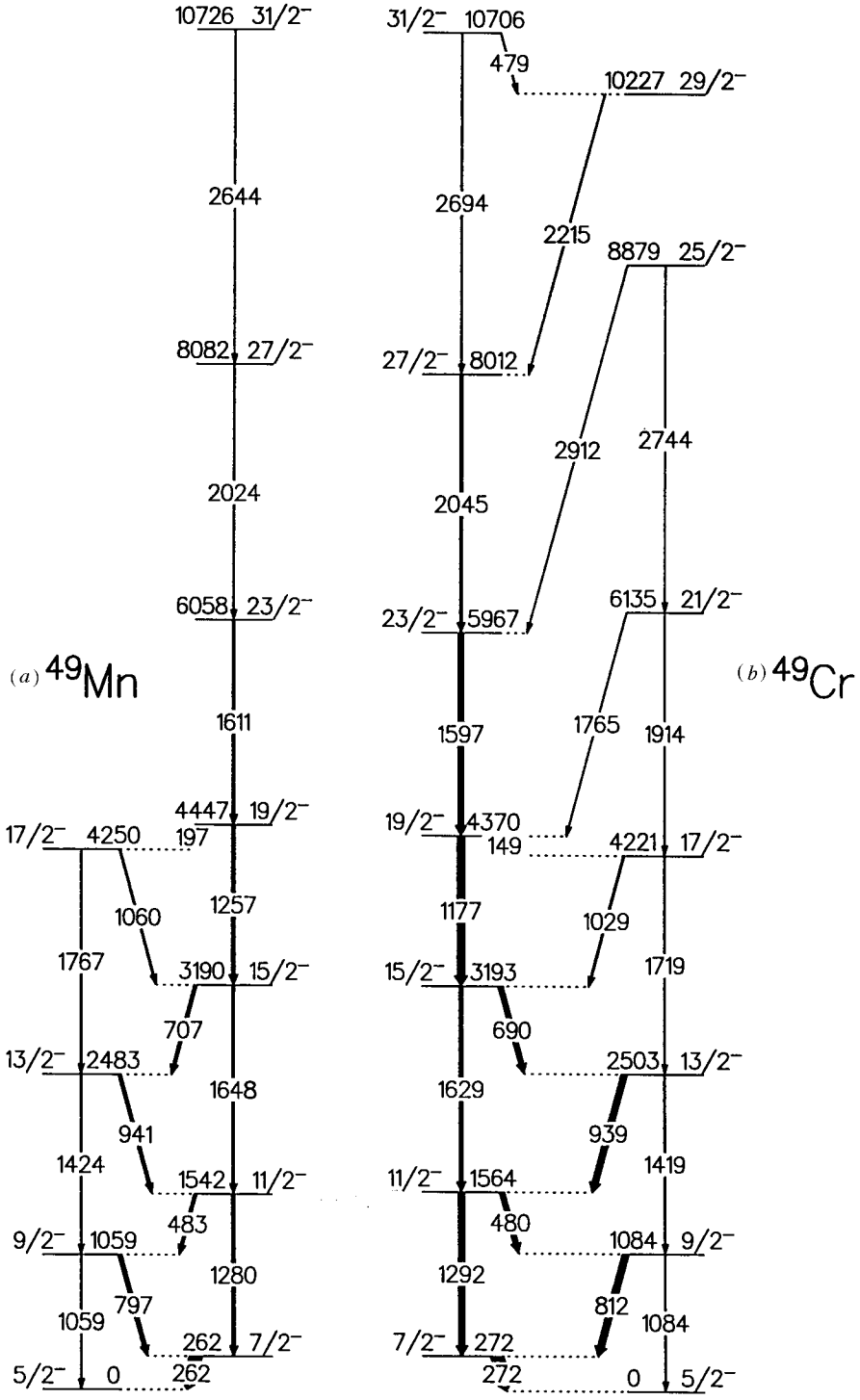

Figure 7. The level schemes of the mirror nuclei $^{49}_{25}\mathrm{Mr}_{24}$ and $^{49}_{24}\mathrm{Cr}_{25}$ (O'Leary *et al.* 1997).

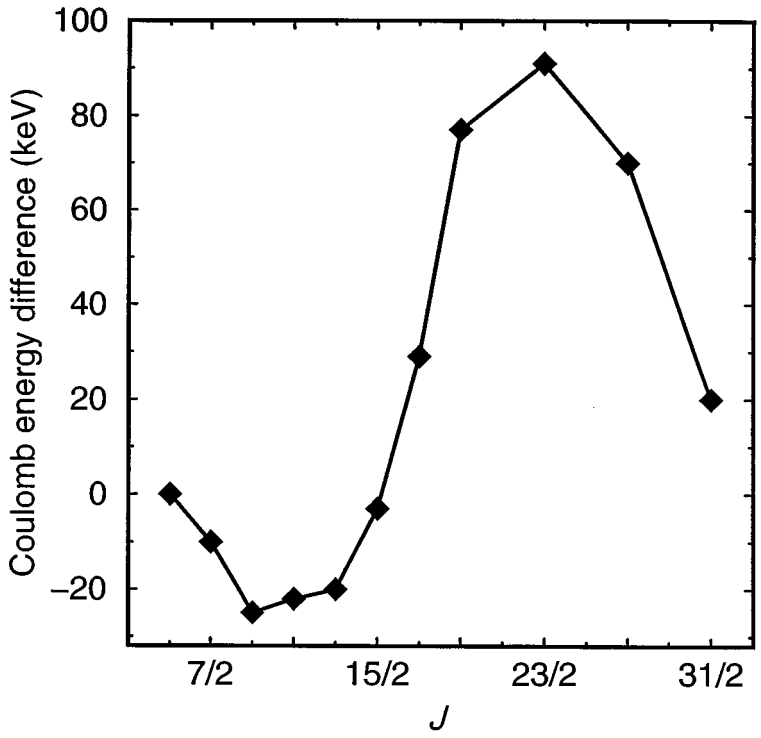

Figure 8. The Coulomb energy difference in kiloelectronvolts for the mass-49 mirror pair (O'Leary *et al*. 1997) as a function of angular momentum along the yrast bands.

be seen in γ-decays; in a $T_Z = 0$ nucleus there should be no $E1$ transitions between $T = 0$ states. Measurements on such nuclei have only been made up to ^{64}Ge (Ennis *et al*. 1991). $E1$ transitions between $T = 0$ states are seen. The results obtained so far are consistent with the theoretical predictions.

Figure 4 shows the limits reached in these experiments. To date most of them have been carried out in studies of the 2n reaction channel with the γ-rays being tagged by detecting the recoiling nuclei and determining their A and Z with a recoil mass separator (James *et al*. 1988). This strategy has the merit that Z identification is eased because the nucleus of interest has the largest Z. At the same time the bombarding energy is kept as close to the Coulomb barrier as possible in order to minimize the number of open reaction channels. The disadvantage is that the reaction cross-sections are very low; in the ^{28}Si(^{58}Ni, 2n)^{84}Mo reaction it is measured to be 7(3) μb. It is also a small fraction of the total cross-section. This sets the experimental limits seen in figure 4. Channel selection using pseudo-4π arrays of charged-particle detectors and the use of more powerful γ-ray arrays will allow us to push these limits further. A good example of the sensitivity of such techniques, albeit a special case, is the recent study by Gorska *et al*. (1997) of the decay of the $(\pi g_{9/2})^{-2}$ isomer in ^{98}Cd. Here the reaction ^{58}Ni + ^{46}Ti was used to create the isomer. The recoiling nuclei were caught on a Nb foil viewed by two EUROBALL cluster detectors with $\varepsilon_{\mathrm{ph}} \sim 6\%$ at 1.3 MeV. The γ-rays from the decay of the isomer were tagged with the reaction channel by the detection of neutrons in a wall of liquid scintillation detectors covering 2π and of charged particles detected in the 4π Si ball. The authors conclude

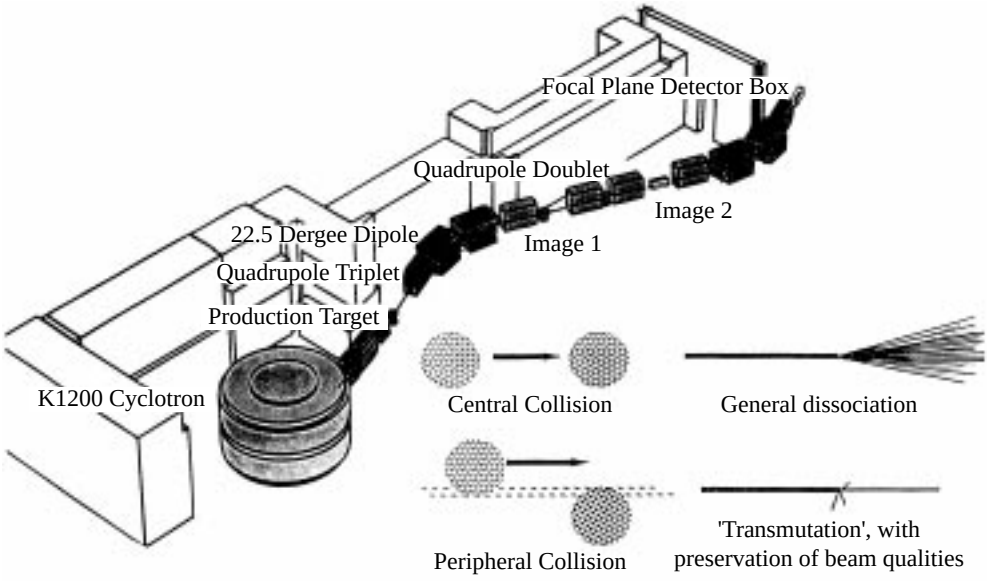

Figure 9. A schematic diagram of the A1200 spectrometer at MSU. The lower right-hand corner shows a simple picture of what happens in high-energy nuclear collisions. In central collisions there is general dissociation, but in peripheral collisions projectile-like fragments are formed which can be refocused and passed through a spectrometer like the A1200.

that the isomeric decay is likely to be from the 8^+ state of the configuration due to two-proton holes in ^{100}Sn. However, the effective charge,

$$e^{\pi} = 0.85 \begin{pmatrix} +20 \\ -10 \end{pmatrix} e,$$

is not consistent with current theories. This shows the power of such methods, which were also used by De Angelis *et al*. (1998) to study ^{72}Kr (figure 5). Real advance requires the advent of intense beams of radioactive ions, which will allow the production of more neutron-deficient compound nuclei. Coupled with the use of sensitive methods of channel selection we can expect to push well beyond the limits shown in figure 4.

(*c*) *Fragmentation studies of* $N \sim Z$ *nuclei*

Studies with fragmentation reactions have provided us with a great deal of information on the existence and properties of $N \sim Z$ nuclei over the past few years. Figure 9 shows in schematic form how fragmentation reactions proceed. In central collisions at energies well above the Coulomb barrier the nucleus breaks up into many pieces, i.e. there are many different reaction products. In peripheral collisions, as shown in figure 9, it is common for projectile-like fragments to survive and continue with the momentum of the projectile in the forward direction. Such fragments will have the N/Z ratio appropriate to nuclei with mass close to the projectile mass. The projectile-like fragments can be refocused and passed through a spectrometer (Sherrill *et al*. 1991) such as the A1200 spectrometer at MSU shown in figure 9. Similar techniques are employed at RIKEN, GSI and GANIL.

The A1200 spectrometer will serve as an exemplar. Energetic heavy ions, typically with energies of 50–100 MeV u^{-1} or even greater, are focused on a thick target. Fragments produced in peripheral collisions, with a linear momentum close to that of the beam particles are focused at various points through the spectrometer. Measurements of the fields in the magnets combined with the position of an ion at the dispersive focal point marked Image 2, measured with a position-sensitive, parallel plate avalanche counter allow the determination of magnetic rigidity $B\rho$. At the final achromatic focus, an Si detector telescope is used to give two energy loss signals and a total energy signal. These measurements, when combined with the measured time of flight (TOF) over a distance of 14 m, from Image 1 to the first element of the detector telescope, give a unique measure of Z and A for each ion.

Figure 10 shows a plot of TOF versus the energy loss ΔE for the products from a natural Ni target bombarded with ^{92}Mo ions of energy 60 MeV u^{-1} at GANIL and analysed with the LISE3 spectrometer. The primary beam intensity was 1.7×10^{10} pps on average. Each cluster of points on this plot represents an individual nucleus of unique A and Z. The observation of such a cluster indicates that the nuclear species lives long enough to survive the flight time of *ca.* 480 ns through the spectrometer. In this particular experiment (Chandler *et al.* 1997), the $T_Z = -1/2$ isotopes ^{77}Y, ^{79}Zr and ^{83}Mo were observed for the first time. The crowning achievement so far with this type of experiment was the observation (Schneider *et al.* 1994; Lewitowicz *et al.* 1994) of the doubly magic nucleus ^{100}Sn, the heaviest known $N = Z$ nucleus. In later measurements its mass has been measured crudely (Chartier *et al.* 1996). A more precise value of the mass is important. The energy of the first excited state is also urgently sought, but this is a very difficult measurement. Doubly magic nuclei such as ^{100}Sn provide benchmarks for the shell model, and the study of the properties of neighbouring nuclei provides the raw experimental information on single-particle energies and two-body residual interactions which underlies shell-model calculations.

In recent experiments (Chandler *et al.* 1997), the techniques of γ-ray and β-ray spectroscopy have been used to study the β-decay and the decay of isomeric levels of fragments which are long enough lived to have survived passage through the LISE3 spectrometer (Mueller & Anne 1991). On the right of figure 10 we see the same plot as on the left but with the additional experimental demand that a γ-ray is detected in one of a set of Compton-suppressed Ge detectors placed in close geometry round the Si detector telescope in which the reaction products are brought to rest. This plot clearly reveals the presence of γ-decaying isomers in some of the transmitted nuclei. Figure 11 shows the γ-ray spectrum associated with ^{76}Rb fragments. They correspond to the γ-rays from the decay of a well-known isomer in this nucleus and reassure us that the method works.

Among the new isomers observed is the unusual case of a 42(8) ns isomer in ^{74}Kr. Figure 12 shows the associated γ-ray and time spectra. What we see is the 456 keV, 2^+–0^+ transition in ^{74}Kr. The 2^+ level has a lifetime of 25 ps (Bonche *et al.* 1985). With this lifetime of 42 ns the nucleus should not survive passage through the LISE3 spectrometer in its isomeric state. The only possible interpretation is that the isomeric level is a 0^+ state lying within 60 keV of the 2^+ state, which decays predominantly via EO conversion to the ground state. If the ions are fully stripped of electrons, the EO transition cannot occur and the effective lifetime in flight will be dictated by the 0_2^+–2_1^+ γ-ray branch. When it stops in the Si detector the nucleus will quickly be clothed in electrons and the decay will revert to the normal lifetime

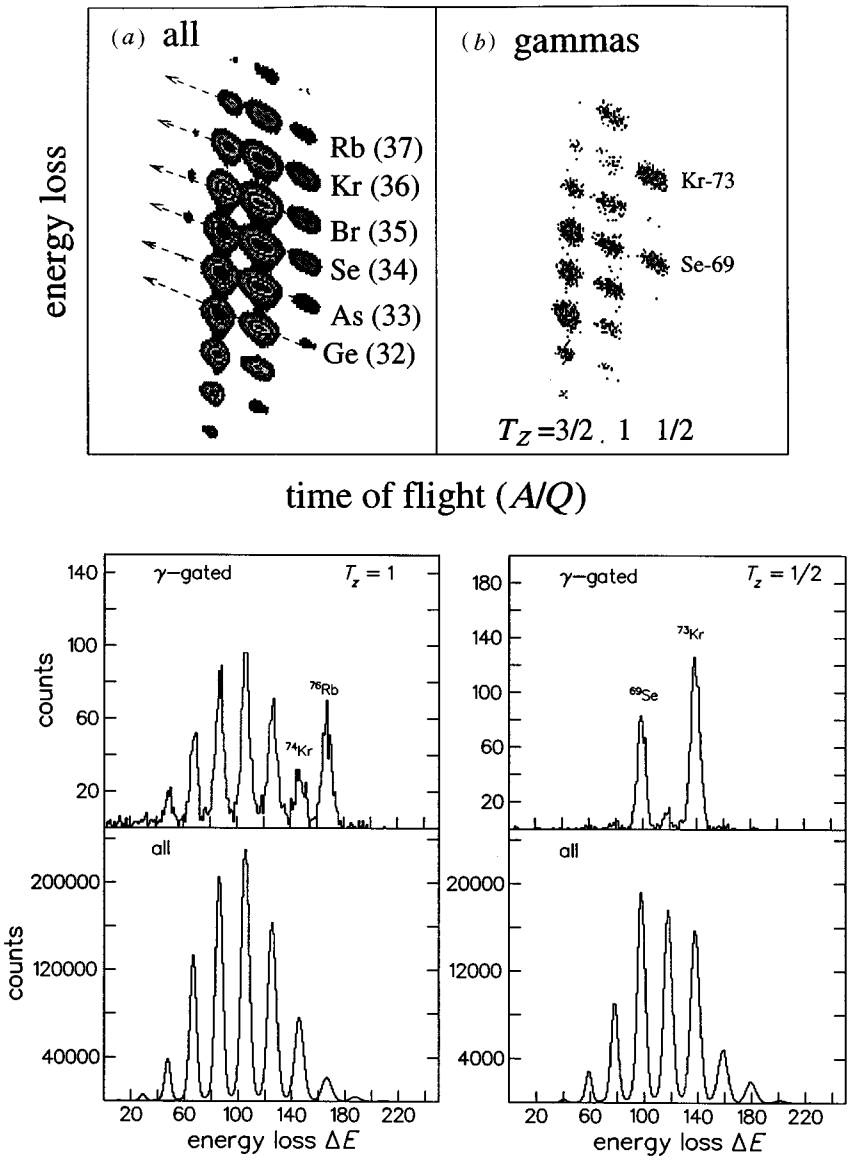

Figure 10. In the upper half of the figure we see (*a*) time of flight versus the energy loss ΔE for the products from a natural Ni target bombarded with ^{92}Mo ions of energy 60 MeV u^{-1} (Chandler *et al.* 1997); (*b*) the same plot but with the additional experimental demand that a γ-ray is detected in one of a set of Compton-suppressed Ge detectors placed round the Si detector telescope where the reaction products are brought to rest. In the lower half of the figure we see a series of projections of these plots.

of 42 ns. The results are interpreted in terms of the coexistence of states of large prolate and oblate deformations in ^{74}Kr. This is consistent with the results of calculations using various models (Bonche *et al.* 1985; Petrovichi *et al.* 1983; Heese *et al.* 1991). Improvements in the intensities of beams produced in fragmentation will greatly enhance the sensitivity of such experiments.

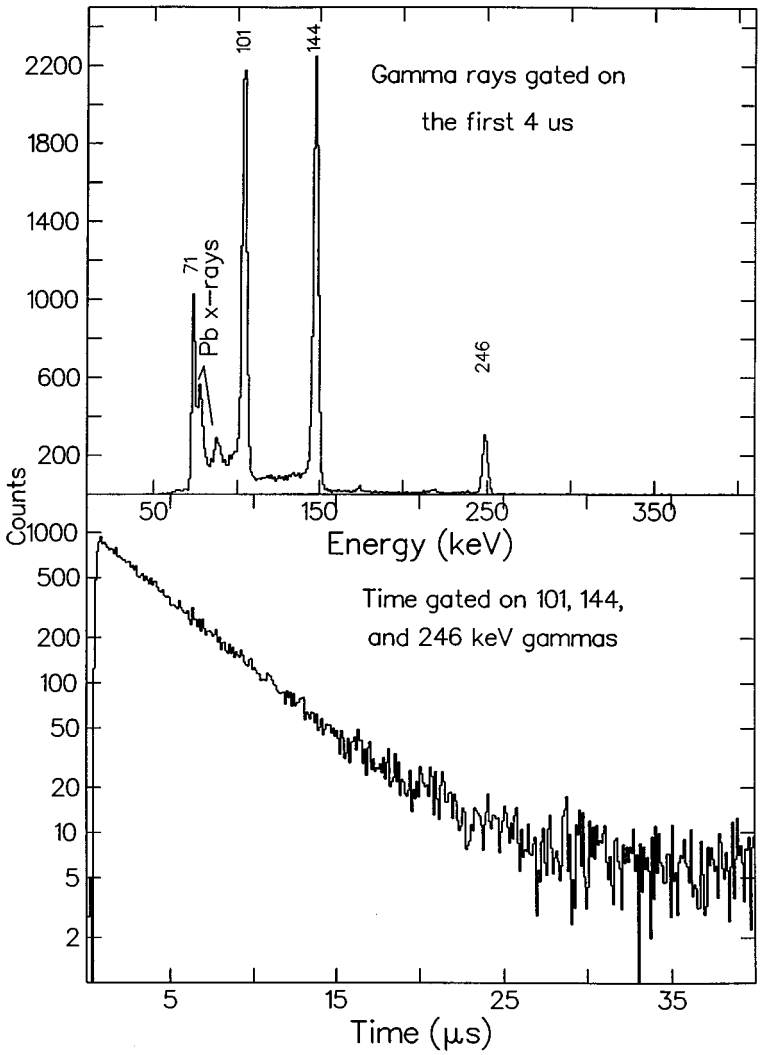

Figure 11. The upper part shows the γ-ray spectrum from ^{76}Rb fragments produced in the bombardment of natural Ni with ^{92}Mo ions of energy 60 MeV u^{-1}. The lower part shows the associated time spectrum.

3. The proton drip-line

(*a*) *Introduction*

We have known that there are limits to the existence of nuclei for a long time. Among these limits we believe that there are minimum and maximum numbers of neutrons which can be supported in a nucleus with a given number of protons if the nucleus is to be energetically stable against the emission of a constituent nucleon. The neutron drip-line arises due to a delicate balance between the (negative) nuclear volume energy and the (positive) asymmetry energy. A large excess of neutrons is necessary before nuclei in their ground-states can decay by emitting a neutron. In contrast, nuclei with too few neutrons can become unbound to the emission of a

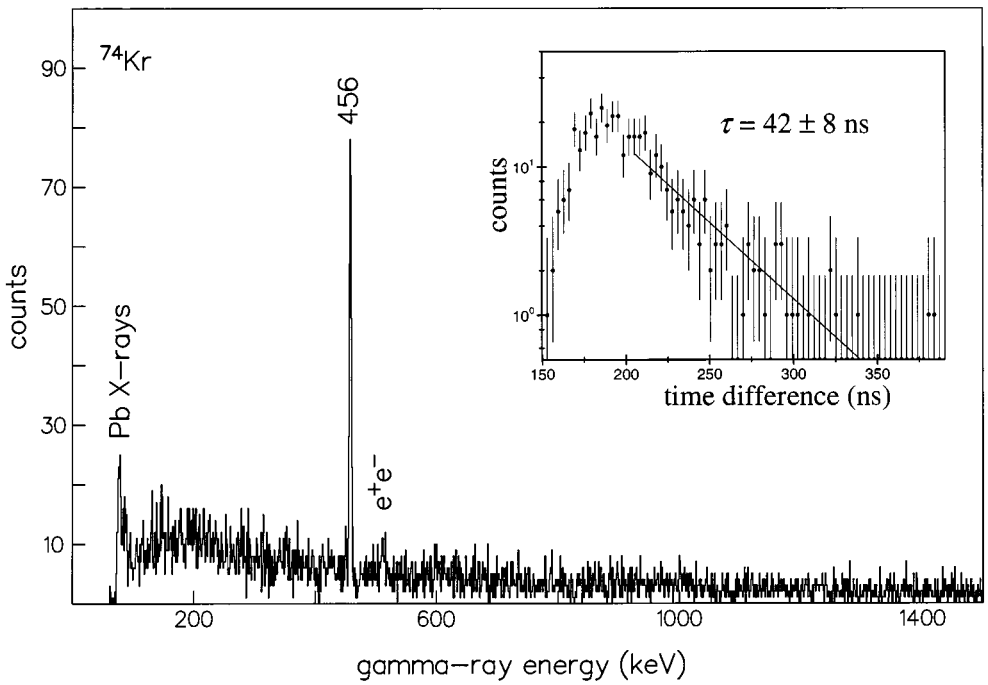

Figure 12. Gamma-ray and time spectra for ^{74}Kr showing the decay of a proposed O^{+} isomer (Chandler *et al.* 1997).

proton. This arises due to the additional effect of a decrease in the electrostatic potential energy.

Consequently, heavy nuclei having more neutrons than protons can be proton-unbound in their ground states. A further important effect of the Coulomb force is that the proton drip-line is much closer to stability than the neutron drip-line. Thus the lightest particle stable F ($Z = 9$) nucleus is ^{17}F whereas the heaviest is ^{31}F; ^{19}F being the only stable isotope. The neutron drip-line has only been established experimentally as far as the fluorine isotopes. Until relatively recently, we could not even be sure that there was a neutron drip-line in heavier nuclei. Myers (1990) considered this problem in the framework of a Thomas–Fermi model of nuclei. On this basis he compared the model predictions with the observed neutron drip-line for light nuclei. Although one must be cautious about such a comparison, since the properties of light nuclei are dominated by surface effects, his tentative conclusion was that neutron matter is unbound. As a result the neutron drip-line must exist, although estimates of where it lies, based on various versions of the semi-empirical mass formula, show enormous variation. In contrast, the relative proximity of the proton drip-line has enabled large swathes of it to be charted. The properties of nuclei lying in the region of the proton drip-line will be outlined below.

(*b*) *The light nuclei*

Nuclear structure and nuclear astrophysics are inextricably intertwined disciplines. Although customarily nuclear structure information is used to illuminate (literally) astrophysical scenarios, what is often overlooked is the role astrophysics studies can

play in understanding nuclear structure. The example of the ^{16}O(p, γ)^{17}F reaction is particularly illustrative. This reaction was shown by Rolfs (1973) to lead to the break-out of the carbon–nitrogen–oxygen (CNO) cycle, which is the main source of energy in massive, high-metallicity stars. In particular, it was found that there was enhanced proton p-wave capture to the continuum which was strongly coupled to a 495 keV, $1/2^+$ excited state in ^{17}F. This is now thought to be associated with an extended tail in the proton wavefunction of this state, which is bound by only 105 keV. Enhanced $E1$ transitions can arise when there is a separation between the centre of charge and mass of the nucleus due to an underlying cluster structure in the wavefunction. Further support for this hypothesis came from studies of the β-decay of ^{17}Ne which revealed a significant enhancement in transitions to the excited state in ^{17}F when compared with the mirror β-decay transition from ^{17}N to ^{17}O (Borge *et al*. 1993). The rapid de-excitation of the excited state by γ-emission prevents the use of radioactive beams for studying the structure of this state directly in nuclear reactions. However, experiments of this type have been used to identify several examples of neutron halo nuclei.

In these cases one or two loosely bound neutrons form an extended matter distribution largely distinct from a core of more tightly bound nucleons. The combined effect of the low binding energy of valence neutrons in nuclei on the border of the neutron drip-line and the short range of the strong interaction results in a high probability of the particles being found deep inside the classically forbidden region, i.e. a long way from the core. In contrast, ground-state proton halos probably only exist in light nuclei near the proton drip-line owing to the attenuating effect of the long-range Coulomb interaction. Searches for proton halos by using radioactive beams will be discussed in § 4.

The proton drip-line is now fully established up to $Z = 21$. In this region the Coulomb barrier is low and hence no proton-unbound nuclei have been directly observed in this region. However, proton-unbound systems such as ^{12}O, ^{15}F, ^{16}Ne and ^{19}Na have been studied in direct reactions, such as (^{3}He, ^{8}Li) (Benenson *et al*. 1975), (^{4}He, ^{8}He) (Kekelis *et al*. 1978), and (π^+, π^-) (Holt *et al*. 1977). Although the nuclei involved can only exist as short-lived resonances, one can detect the stable ejectile, and the kinematics of the two-body system allow one to determine the ground-state mass and excited state of the unstable system. The masses of light, proton-unbound nuclei have been shown to deviate systematically from nuclear mass relations based on the charge independence of the nuclear force (Comay *et al*. 1988). This effect is thought to arise from changes in the Coulomb potential energy in the intrinsic wavefunctions of the unbound systems. Short-lived resonances beyond the proton drip-line may play a role in nucleosynthesis via the rapid proton capture rp-process. It has been suggested by Görres *et al*. (1995) that two-proton capture may bridge the gaps in the rp-process pathway which occur at proton-unbound, odd-Z nuclei. They suggest that the ^{38}Ca(2p,γ)^{40}Ti reaction will act to bridge the gap across ^{39}Sc if the temperatures and densities in X-ray bursters are high enough.

The rp-process (Wallace & Woosley 1981) may proceed in certain astrophysical scenarios all the way along the proton drip-line up to ^{100}Sn. It is thus important to establish the limits of particle stability which will act as a constraint on the path of nucleosynthesis. In particular, the instability of certain isotopes can lead to waiting points in the process, which are dictated by long-lived β-decays. This can cause the rp-process to be impeded or even fizzle out completely.

The mapping of the proton drip-line from $Z = 21$ to $Z = 50$ has gone ahead in leaps and bounds in recent years, largely due to the type of fragmentation studies described earlier (Chandler *et al*. 1997). The key point is that nuclei observed in these studies have a lifetime longer than the flight times through the separators, which vary from 0.1 to 5 μs, and these times are much shorter than the shortest β-decay half-lives. In essence we have now mapped out the drip-line for all odd-Z nuclei up to In ($Z = 49$). For example, recent experiments have shown that the $T_Z = -1/2$ nuclei ^{69}Br and ^{73}Rb (Pfaff *et al*. 1996; Blank *et al*. 1995) are proton unbound. In the latter case the failure to observe the radioactive decay of this nucleus at ISOLDE, where it is produced in proton spallation, had already suggested this (D'Auria *et al*. 1977). At the same time the heavier $T_Z = -1/2$ nuclei ^{77}Y and ^{89}Rh have been observed at GANIL (Chandler *et al*. 1997). The explanation must lie in the changes in both overall deformation and the orbits involved. The rapidly changing nuclear structure in this region of the drip-line, and its effect on nuclear masses, etc., must be taken into account in theoretical models of the rp-process. Furthermore, important information is required on β-decay half-lives, and β-delayed proton emission branches. For example, the β-decay half-life of the $T_Z = -1/2$ nucleus ^{65}As has been determined at MSU by using the A1200 fragment separator (Winger *et al*. 1993). Valuable information has also been obtained from traditional on-line separators. For example, the β-delayed proton emission of ^{94}Ag has been studied (Schmidt *et al*. 1994) at the GSI on-line separator.

(*c*) *Beyond* $Z = 50$*: studies of proton radioactivity*

For nuclei in the region of the proton drip-line with $Z > 50$, the Coulomb barrier experienced by an unbound valence proton is substantial (see figure 4). This barrier will retard proton emission. Hence, heavy nuclei beyond the proton drip-line can exist in relatively long-lived, quasi-stationary states before radioactive decay occurs. This phenomenon is known as proton radioactivity. In contrast to the long-known and well-studied decay mode of α-emission, no clustering preformation factor is necessary since the proton is a pre-existing constituent of the nucleus. The Coulomb barrier experienced by the proton is relatively low, due to its smaller charge, and hence lower decay energies are required for tunnelling to take place. A further important distinction is that the mass of the proton is lower, which leads to a relatively high centrifugal potential for non-s-wave states (see figure 13). This produces a high sensitivity of the tunnelling probability, and hence of the half-life, to the orbital angular momentum of the emitted proton. As a result, proton-decay energy and half-life measurements can be used to determine the proton shell ordering beyond the drip-line by a comparison with simple Wentzel–Kramers–Brillioun (WKB) calculations. Deviations from these calculations may be evidence of nuclear structure effects such as deformation and configuration mixing.

Due to the unsuitability of primary beam species, fragmentation reactions cannot presently be used to access this region of the proton drip-line. All successful measurements of ground-state proton radioactivity have used heavy-ion-induced, fusion–evaporation reactions. Cross-sections have varied from tens of microbarns for 1p2n evaporation channels to around 10 nb for the 1p5n channel. The most successful method of identifying proton-emitters has involved the in-flight separation of fusion–evaporation reaction products before implantation into a silicon detector. This was

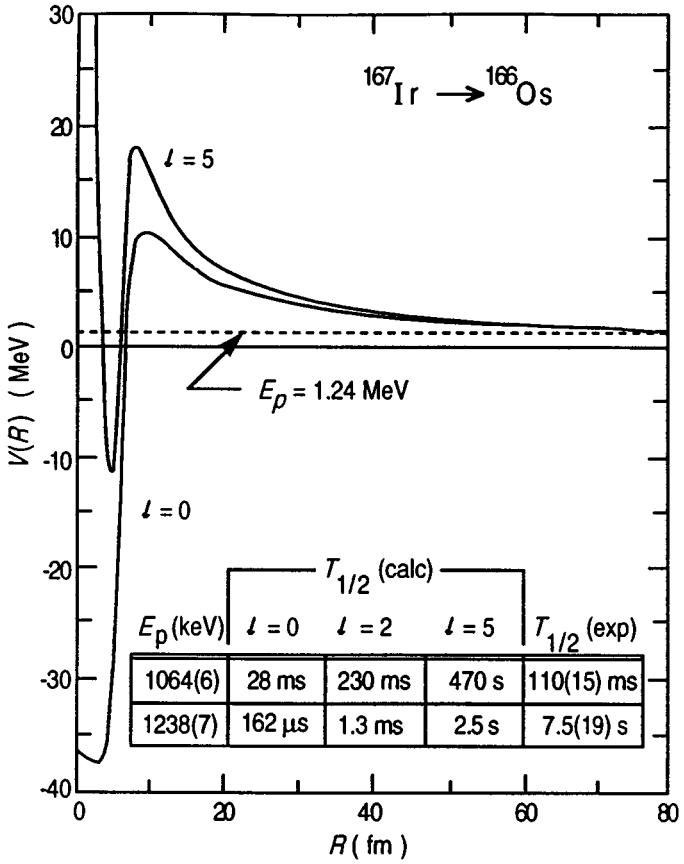

Figure 13. An illustration of the potential energy barrier, due to the superposition of Coulomb and centrifugal potentials, faced by the odd valence proton emitted by the ground-state proton emitter ^{167}Ir. The inset shows the dependence of the half-life for two-proton branches on the orbital angular momentum (l) of the proton.

the method employed in the discovery of the first ground-state proton emitter ^{151}Lu by using the velocity filter SHIP at GSI in 1981. The 1990s saw a dramatic increase in the number of known examples of ground-state proton radioactivity, due to work using the recoil mass separator (RMS) at Daresbury (James *et al*. 1988) and latterly the fragment mass analyser (FMA) at Argonne (Davids *et al*. 1992) (see figure 14). In both cases, in-flight velocity/energy separation of slower-moving evaporation residues and the unreacted beam particles at 0° is followed by a magnetic dipole section which disperses ions according to their mass number-to-charge state ratio, A/q. The mass dispersion at the focal plane of the separators can be used to select and identify ions of the required mass. The Edinburgh group developed a double-sided silicon strip detector (DSSD), which consisted of 48 × 48 orthogonal Si strips on the front and back with strip widths of 300 µm into which ions were implanted (Sellin *et al*. 1992). The subsequent decays were correlated in time and position in order to enhance the selection of short-lived radioactivities such as proton decays. In many instances, proton emission was followed by known α-decay chains, in which case correlations between decays could be used to obtain very high detection sensitivities.

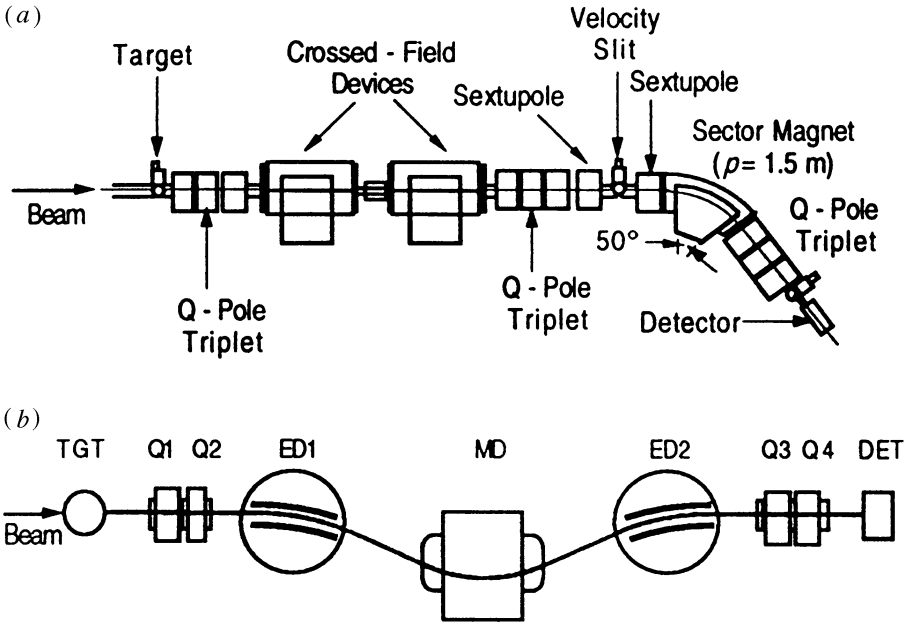

Figure 14. Schematic diagrams of (*a*) the Daresbury Recoil Separator (James *et al*. 1988) and (*b*) the fragment mass analyser at the Argonne National Laboratory.

Proton radioactivity has now been established for all odd-Z elements from Ho ($Z = 67$) to Bi ($Z = 83$) (Woods & Davids 1997). These data have enabled us to study systematically the factors affecting the proton-decay transition probability. In particular, it has been shown that proton-decay spectroscopic factors agree very well with the trends predicted by a shell-model-based calculation for spherical nuclei lying between the $Z = 64$ and $Z = 82$ shells (Davids *et al*. 1997). The recent discovery of proton radioactivity from ^{141}Ho by using the FMA has provided an exciting counter-example. Here the measured proton-decay rate gives a spectroscopic factor in dramatic disagreement with this calculation. However, a macroscopic–microscopic mass model calculation predicts that large quadrupole deformations ($\beta \approx 0.3$) set in below $Z = 68$ in the region of the proton drip-line (Möller *et al*. 1997). It had been shown earlier (Lister *et al*. 1985) that a region of deformed nuclei existed, which centred on $N = Z = 64$. Calculations using a deformed Nilsson wavefunction basis have been able to reproduce anomalously low spectroscopic factors for the nuclei ^{109}I and ^{113}Cs assuming relatively modest deformations ($\beta \approx 0.1$). Following this approach, a good agreement can also be obtained for the ^{141}Ho decay assuming $\beta \approx 0.3$ (Davids *et al*. 1998). Such studies provide an insight into the fragmentation of single-particle strength within the Nilsson basis. For a comprehensive study of the effects of deformation on the proton-decay rate, one wishes ideally to determine the ground-state deformations independently. As indicated earlier this can be achieved by studying the de-excitation γ-rays feeding the ground states. Such nuclei are, of course, especially difficult to study in this detailed manner as they reside at the very limit of stability. A technique for identifying γ-ray transitions in heavy, neutron-deficient nuclei is discussed in the following section.

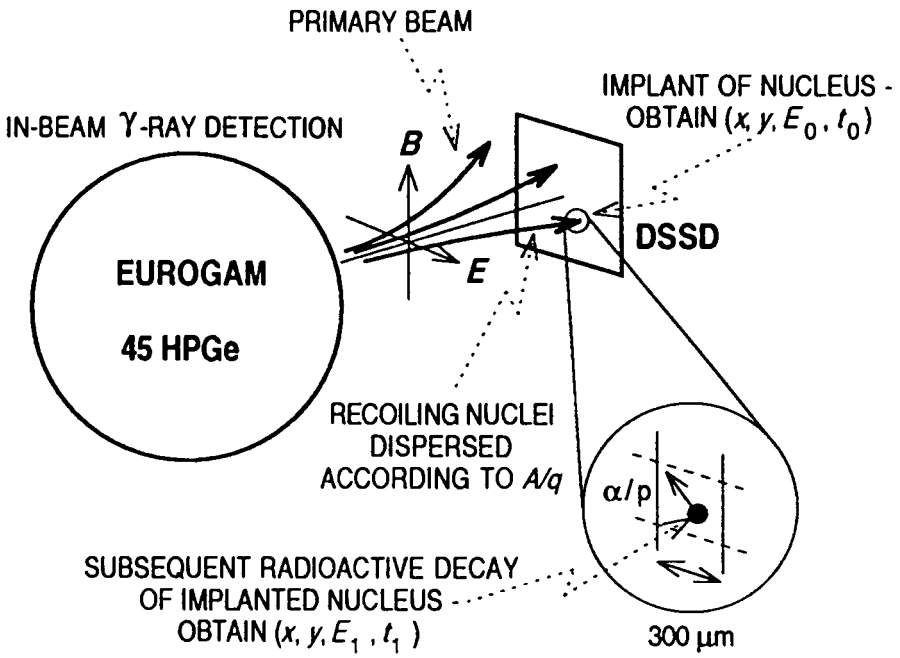

Figure 15. The principle of the RDT method (Paul *et al*. 1995). (See text.)

(*d*) *Gamma-ray spectroscopy at the proton drip-line by using recoil decay tagging*

The proton-decay studies described above provide information about the ground state and a few isomeric states in proton-unstable nuclei. Information on excited states in these nuclei is also required. However, the technique employed to identify γ-rays from nuclei such as ^{84}Mo cannot be applied here since the resolution of gas-ionization detectors is not sufficient to resolve isobars of slow-moving, heavy nuclei with $v/c \leqslant 2\%$. The recoil decay tagging technique, RDT, (see, for example, Seweryniak *et al*. 1998), based on the proton-decay studies, has allowed us to observe and assign prompt γ-rays in many highly neutron-deficient, heavy nuclei. It relies on the ground-state radioactive decay of a nucleus having a unique signature, a kind of genetic finger-printing for γ-rays.

Figure 15 shows how the method works. The target is surrounded by an array of Compton-suppressed Ge detectors, which detect the prompt γ-rays emitted in high multiplicity from the target. The recoiling nuclei from the thin target are separated from the beam particles by a recoil separator.

They are then implanted into a DSSD, where their decays are recorded. All of the signals are tagged with a clock pulse, so that it is possible not only to correlate subsequent decays with the arrival of the implanted ion, but with the coincident in-beam, γ-rays detected at the target. If one is populating nuclei far from stability, a large number of α-emitters or ground-state proton emitters are populated. The resulting α-spectrum is complex as we see in figure 16, but software gates set on the appropriate α- or proton-peak allows clear channel selection. In essence the recoil separator acts principally to separate beam particles from recoils, and the identification and assignment are made on the basis of the particle decay energy and the decay lifetime.

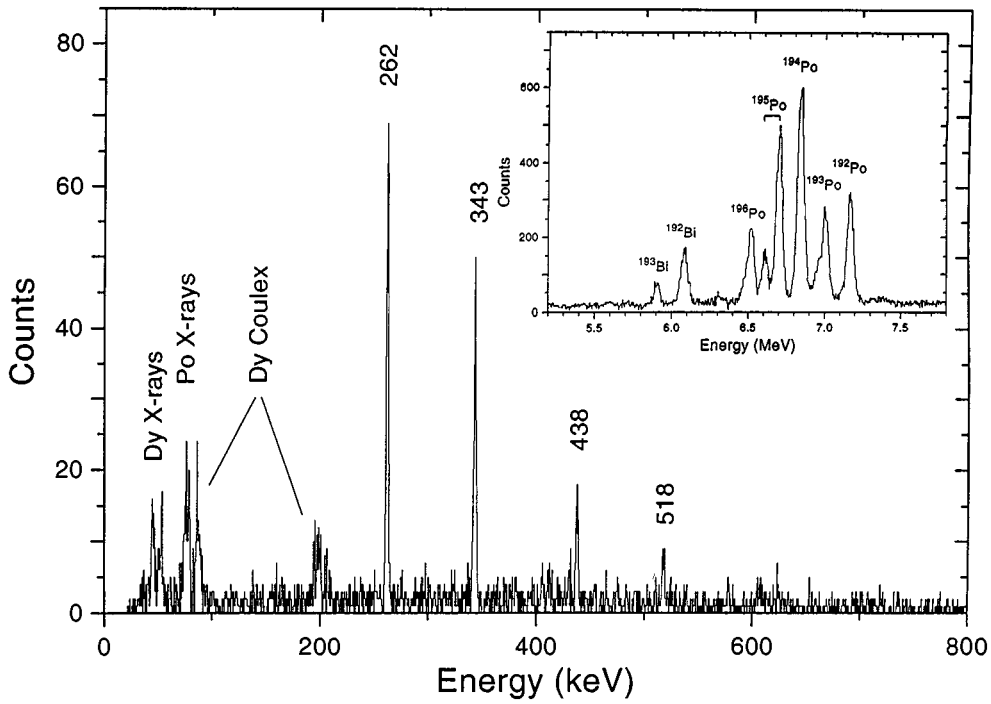

Figure 16. An example (Helariutta *et al*. 1996) of the γ-ray spectrum from ^{192}Po obtained with the RDT technique. In this case the ^{192}Po γ-rays were tagged by gating on the ^{192}Po α-particles.

This basic technique was first applied by using a NaI array coupled to the velocity filter SHIP at GSI in order to study heavy-ion radiative capture by identifying the α-decay of ^{180}Hg (Simon *et al*. 1986). The low resolution of the NaI array limited the sensitivity of the technique, and it was not until the advent of high-efficiency, high-resolution γ-ray arrays that the full power of the RDT technique became apparent in later independent work using the Daresbury RMS (Paul *et al*. 1995). In this case the Eurogam Ge detector array ($E_{\mathrm{ph}} \approx 4.5\%$ for a 1 MeV γ-ray) was used for γ-ray detection in a parasitic experiment. In-beam γ-rays from a proton emitter, ^{109}I, were identified for the first time and β-delayed proton- and α-correlations were used to identify γ-rays from several other neighbouring nuclei. In later RDT work using the Argonne FMA, γ-rays were identified from the ground-state band of the proton emitter ^{147}Tm, providing an indication of the ground-state deformation for the first time (Seweryniak *et al*. 1998). In this same experiment it was also shown that isomeric proton decays could be used to provide a tag on the feeding of states within a nucleus other than the ground state.

High-efficiency gas-filled separators such as RITU at Jyvaskyla are particularly powerful devices for studying very heavy nuclei produced in regions where the compound nucleus primarily decays by fission. This is because they separate recoils from beam particles cleanly and transmit the recoils with high efficiency. Figure 16 shows the results of just such an experiment (Helariutta *et al*. 1996). Here the γ-rays from the ^{160}Dy(^{36}Ar,4n)^{192}Po reaction were identified by gating on the peak from the α-decay of ^{192}Po. Here the γ-ray array had an efficiency of *ca.* 0.6% for 1.3 MeV γ-rays. The estimated efficiency for detecting the ^{192}Po recoils was 25%, and about 50% of

the particles emitted by them was detected. The cross-section for this reaction was estimated to be *ca.* 10 μb.

4. The use of radioactive beams

(*a*) *Spectroscopic studies of neutron-deficient nuclei using radioactive beams*

How can we expect the use of radioactive beams to improve or alter the experimental situation described earlier?

First, it will be possible to use beams of neutron-deficient radioactive ions to study the structure of these radioactive species and their near neighbours in Coulomb excitation and transfer reactions.

The usefulness of Coulomb excitation is clear from a few examples. We have established that nuclei close to ^{76}Sr and ^{80}Zr (Lister *et al*. 1990) and the light, rare-earth nuclei (Lister *et al*. 1985) centred on $Z = N = 64$ are highly deformed in their ground states. The evidence for this is largely based on measurements of $E(2_1^+)$ for the even–even nuclei, with the corresponding deformation being derived from empirical relationships (Raman *et al*. 1991; Grodzins 1966) between $B(E2; 2_1^+–0_1^+)$ and $E(2_1^+)$. A direct measurement of the $B(E2)$ in Coulomb excitation would be much more convincing.

Depending on whether the lifetime of the state is nano- or picoseconds, one can readily envisage at least two straightforward methods of measuring the $B(E2)$. If the lifetime is short, then γ-ray emission will occur in or very close to the target. As a result, a measurement of the total γ-ray yield per projectile will allow us to extract the $B(E2)$. If the lifetime is longer, and a thin target is used, the nucleus will recoil out of the target. It should then be possible to measure directly the lifetime of the state involved by determining the number of γ-rays emitted as a function of distance from the target. Given the large cross-sections for Coulomb excitation, it should be possible to make meaningful measurements with beams of only 10^3–10^4 ions per second. Beams of this intensity are already available from the fragmentation process. Although the high velocity of the fragments brings its own problems, measurements of $B(E2; 2–0)$ have been made successfully for neutron-rich nuclei (F. Asaiez and others, personal communication; Sorlin 1998).

In the same way, charged-particle transfer reactions will provide vital information not only about the energies, spins and parities of states in nuclei far from stability but about the single-particle strength in states in these nuclei. This will be of particular importance for states in the nuclei close to doubly magic ^{100}Sn. The location of such states provides essential input for shell-model calculations.

As noted earlier much of our knowledge of nuclei far from stability has come from studies of γ-rays emitted in fusion–evaporation reactions. The use of radioactive ions will mean more neutron-deficient compound nuclei can be created and there will be enhanced cross-sections for producing very neutron-deficient nuclei. Using radioactive ions inevitably means that there is a considerably increased background in the experiments. Catford *et al*. (1996) have shown that the difficulties can be overcome in studies of the $^{19}\mathrm{Ne} + {}^{40}\mathrm{Ca}$ reaction at 70 MeV. Figure 17 shows the experimental set-up schematically. The beam of $^{19}\mathrm{Ne}^{4+}$ ions at 70 MeV was provided by the coupled CYCLONE accelerator facility (LLN) at Louvain-la-Neuve (Darquennes *et al*. 1990). The γ-rays were detected in seven, Compton-suppressed, Ge detectors placed

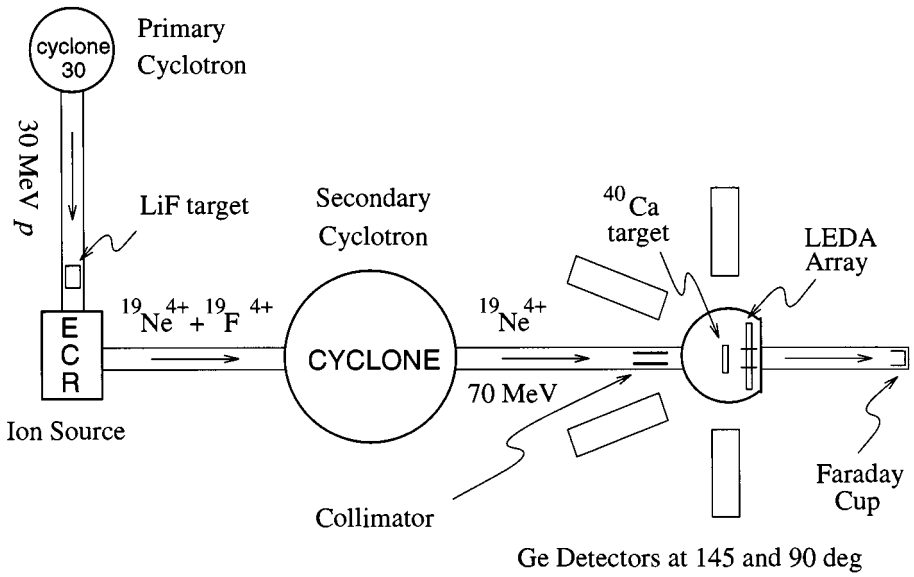

Figure 17. A schematic diagram showing the experimental set-up in the study of the ^{40}Ca+^{19}Ne reaction at Louvain-la-Neuve. The second cyclotron could be tuned to provide either a ^{19}Ne^{4+} beam as shown or a ^{19}F^{4+} beam.

in the backward direction. Charged particles emitted in the reaction were detected in the LEDA array (Coszach *et al*. 1995) of Si annular strip detectors which covered 10% of the solid angle in the forward direction. Given the radioactivity of the beam, care was also taken in shielding the beam collimators and the beam dump with lead. This was particularly important given that *ca*. 5% of the beam was stopped on the final beam collimators, 150 mm before the target.

The data in this experiment were recorded in event-by-event mode including the timing relative to the cyclotron radio-frequency pulses. Figure 18 shows the timing spectra for γ-rays relative to the beam pulse. The upper two panels show the singles- and γ–γ coincidence-spectra relative to the ^{19}Ne beam pulse. The final panel shows the singles spectrum relative to the ^{19}F beam pulse. The peaks are 8 ns wide and 73 ns apart. There is a large difference between the stable and radioactive beam experiments due to the difference of two orders-of-magnitude in the number of particles per pulse and the background from beam radioactivity.

The effect is evident in figure 19, which shows the γ-ray spectra from the ^{19}Ne + ^{40}Ca reaction. Figures 19a, b, d are from 90° detectors and figure 19c is from all detectors. The singles spectrum is dominated by annihilation radiation. The only other peaks seen are from radioactivity induced by a brief irradiation with ^{19}F. The effectiveness of the γ–γ coincidence requirement depends on the detector geometry around the sites of β^+ activity. In terms of producing clean spectra, this is only effective if the average γ-ray multiplicity following β-decay is large. However, the elimination of non-reaction counts from the γ-spectra was achieved by using the measurements of γ-ray timing relative to the beam pulses. The need for this, and the reason for its effectiveness, are clearly evident in figure 18. The spectrum obtained by subtracting the spectrum recorded between beam pulses from one recorded during the

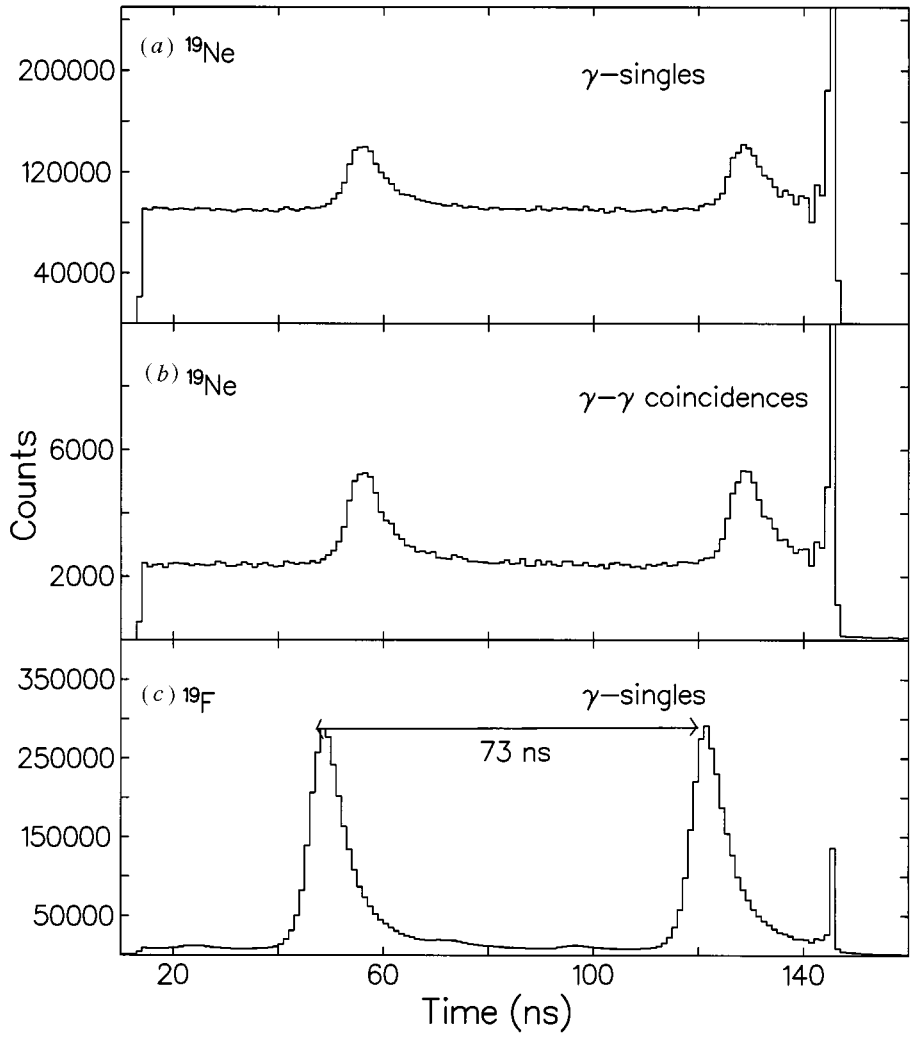

Figure 18. The timing spectra for γ-rays relative to the beam pulse for (a) $^{40}\mathrm{Ca} + {}^{19}\mathrm{Ne}$ singles, (b) $^{40}\mathrm{Ca} + {}^{19}\mathrm{Ne}$ γ–γ coincidences, and (c) $^{40}\mathrm{Ca} + {}^{19}\mathrm{F}$ singles. The electronics distributed the true in-beam events evenly between the two peaks for odd- and even-numbered beam pulses. The spike above channel 140 is an artefact of the data.

in-beam peak of the timing spectra is seen in figure 19*d*. The result is a clean spectrum of the prompt γ-rays which are produced in the fusion–evaporation reaction.

The main conclusion is that active Compton suppression with bismuth germanate shields gave data of comparable quality to that of stable beams. Gamma-rays down to 100 keV can clearly be studied. The combination of time-to-digital-converter gating and gating on combinations of charged particles is also effective in allowing channel selection. To achieve this, software gating on the beam pulse with background subtraction was essential. This was also essential to obtain clean coincidence spectra. The most important source of background was beam radioactivity which had been stopped on the collimators. The conclusion here must be that good emittance is an

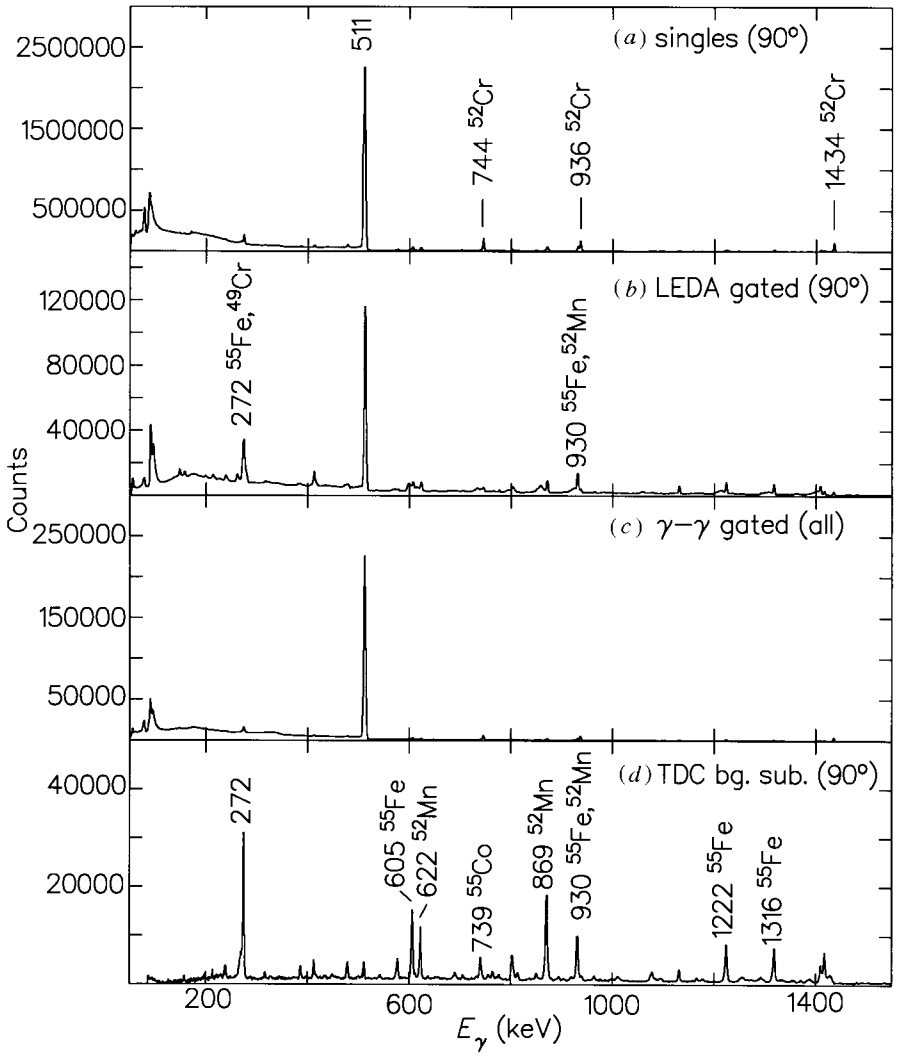

Figure 19. Examples of the γ-ray spectra from the study of the $^{19}\mathrm{Ne} + {}^{40}\mathrm{Ca}$ reaction (F. Asaiez and others, personal communication; Sorlin 1997). (*a*) All singles, (*b*) in coincidence with charged particles, (*c*) in coincidence with other γ-rays, and (*d*) singles with full background subtraction as described in the text. The spectra consist of combined data from all 90° Ge detectors, except (*c*) which includes detectors at 145° as well.

essential requirement for the post-accelerator of a radioactive beam facility, as is a flexible beam structure, if studies of this kind are to prove successful.

Thus it is clear that, given proper attention to beam properties and shielding, one can obtain clean spectra from fusion–evaporation reactions induced by radioactive ions. An example of the effect on our studies is summarized in table 1. Studies of medium mass $N = Z$ nuclei have relied on the 2n-channel in heavy-ion-induced fusion–evaporation reactions, which has a very small cross-section. Radioactive ions will allow us to make more neutron-deficient compound nuclei and hence reach further from stability.

Table 1. *The population of $N = Z$ nuclei with stable and radioactive beams*

reaction	^{58}Ni + ^{12}C	^{34}Ar + ^{40}Ca	^{33}Cl + ^{40}Ca
E_{lab} (MeV)	175	115	110
CN	$^{70}_{34}$Se	$^{74}_{38}$Sr	$^{73}_{37}$Rb
$L_{\mathrm{grazing}}(\hbar)$	14	29	30
σ (mb)	^{68}Se + 2n (0.5)	^{68}Se + α2p (2.5)	^{64}Ge + α2p (7)
		^{64}Ge + α2p (28)	

Improved methods of channel selection and suitably tailored γ-ray arrays will also allow us to use stronger channels such as the α2n channel. As a result, we can contemplate a considerable leap forward in our knowledge of $N = Z$ nuclei.

In terms of studies of heavy, proton-unbound nuclei, the ability to create compound nuclei farther from stability means that we may be able to reach certain nuclei which are presently inaccessible, and improve access to known nuclei via evaporation reaction channels with larger cross-sections such as the p2n rather than the p4n reaction. Even if one uses a beam 10^{-3} times weaker, which compensates a cross-section 10^{-3} times stronger, the sensitivity of the measurement could be improved since the relevant cross-section is a much larger fraction of the total cross-section.

(*b*) *Nuclear reactions along the proton drip-line*

It is only possible to study nuclear reactions along the drip-lines by using radioactive beams. It was pioneering experiments with fragmented radioactive beams at Berkeley that produced the first strong evidence for the neutron halo in ^{11}Li (Tanihata *et al*. 1985). The large interaction cross-section for ^{11}Li ions was associated with an extended matter distribution, which was later assigned to spatially extended wavefunctions of the two loosely bound valence neutrons (Hansen & Jonson 1987). Subsequent break-up reaction studies confirmed the basic correctness of this interpretation (Koboyashi *et al*. 1989). Several further examples of neutron halo nuclei have been identified in this manner, and similar experiments are now being performed to identify ground-state proton halos. These are only expected to occur in relatively light nuclei, where the Coulomb barrier is relatively modest, and for states with low orbital angular momenta.

Interaction cross-section measurements performed at RIKEN on $A = 17$ isobars indicated a modest enhancement for the scattering of ^{17}Ne ions, which was interpreted as a possible halo structure (Ozawa *et al*. 1994). It has subsequently been suggested that a two-proton halo may arise from a large $(\pi s_{1/2})^2$ component in the ^{17}Ne ground-state wavefunction (Zhukov & Thompson 1995). Several experiments have been performed on the nucleus ^{8}B, which has a p-ground-state proton with a very low binding energy of 0.14 MeV (Schwab *et al*. 1995). In this case the experiments have given conflicting interpretations on the existence of a proton halo, and current work is in progress to resolve this issue. The attenuation of the proton wavefunction by the Coulomb force will reduce the spatial extent of the halo in comparison with neutron halos, making the signature of its existence more ambiguous.

Radioactive beams can be used to populate light, proton-unbound nuclei by using simple reaction mechanisms. For example, a fragmented ^{13}O beam was used at MSU to produce the two-proton, unbound ground-state resonance of ^{12}O via the single-neutron stripping reaction (^{13}O,^{12}O) (Kryger *et al*. 1995). The decay of the resonance to a ^{10}C nucleus and two protons was detected and the decay mechanism was studied.

Subsequent work at GANIL using the ^{10}C+p reaction to populate resonances in the proton-unbound nucleus ^{11}N revealed a previously unobserved low-lying resonance (Axelsson *et al*. 1996). These data imply that sequential two-proton emission via intermediate resonances in ^{11}N will probably dominate the ^{12}O decay mechanism. An experiment at the radioactive beam facility at Louvain-la-Neuve used a low-energy ^{13}N beam to populate a resonance in ^{14}O that is unbound to two-proton emission (Bain *et al*. 1996). Coincident protons were detected by using the LEDA silicon strip detector array. A weak, two-proton-decay branch was identified that also decayed predominantly by a sequential mechanism. Searches for a possible ^{2}He decay mechanism are of great interest for the potential insight this may provide into correlations within nuclei. This has become an even more interesting issue with the recent discovery of the dominance of ^{2}He emission in the study of the ^{16}O(e$'$,epp) reaction mechanism at Nikhef (Onderwater *et al*. 1997).

Low-energy radioactive beams produced by ISOL-based facilities such as Louvain-la-Neuve address a distinctively different range of physics issues, and such studies are in a state of relative infancy compared to fragmentation methods. Of particular importance are the direct studies of astrophysically important reactions occurring on light radioactive nuclei. These reactions take place at energies below and around the Coulomb barrier in explosive astrophysical scenarios and are often critically influenced by the characteristics of isolated resonances. Inverse scattering techniques are a particularly powerful method. For example, the p(^{18}F,^{15}O)α reaction has been studied (Coszach *et al*. 1995) at Louvain-la-Neuve by detecting and identifying α-particles by using the LEDA array. This reaction is crucial in determining the astrophysical conditions for the operation and break-out from the hot CNO cycles. The large resonant yields of α-particles suggest that this reaction prevents the production of ^{19}Ne via the ^{18}F(p,γ)^{19}Ne reaction, in which case ^{19}Ne is likely to be produced mainly through the ^{15}O(α,γ)^{19}Ne reaction. It will be very important to measure this reaction since ^{19}Ne is likely to be the break-out point from the hot CNO cycles to the rp-process. An extensive discussion of these processes is described in the accompanying article by Wiescher, Schatz and Champagne (this issue).

One can anticipate exciting advances in reaction studies by using radioactive beams near the Coulomb barrier. Of great interest will be sub-barrier reaction processes such as fusion and transfer studies. In particular, sub-barrier transfer reactions can be used to determine valence nucleon density distributions in the tail of the nuclear wavefunction, in a relatively model-independent way. Such experiments offer an exciting prospect for the detailed study of the properties of halo nuclei.

5. Conclusion

Recent years have seen a rapid and dramatic advance in our knowledge of proton-rich nuclei. The main vehicles for populating these nuclei have been heavy-ion-induced, fusion–evaporation reactions near and above the Coulomb barrier and high-energy fragmentation of heavy ions.

A large portion of the proton drip-line has been mapped out and we have learned much about the $N = Z$ nuclei up to $A \approx 80$. The use of the RDT technique (Paul *et al*. 1995) is beginning to reveal the properties of very neutron-deficient nuclei above ^{100}Sn. The main limitation to these studies is the constraint of using stable ions and stable targets.

Radioactive-ion-beam experiments using classical techniques such as Coulomb excitation and single nucleon transfer will greatly increase our knowledge of the structures of many nuclei far from stability, including neutron-deficient nuclei. In such studies the exotic nucleus is either the beam species itself or a close relation. Proton-rich radioactive beams can also be used to produce highly neutron-deficient compound nuclei, allowing the study of isotopes near the proton drip-line produced via strong charged-particle evaporation channels. In general, such studies will populate distinctly different states from those produced by direct-reaction mechanisms such as single nucleon transfer. This will provide much more comprehensive spectroscopic information than is presently possible with stable-beam experiments.

Nuclear reaction studies with high-energy fragmented radioactive beams can be used to explore the scattering and break-up characteristics of proton-halo candidate nuclei at the proton drip-line. Low-energy radioactive beams enable us to directly reproduce astrophysically important reactions involving proton-rich nuclei thought to occur in explosive scenarios such as novae and X-ray bursters. Reactions involving such loosely bound nuclei may be expected to produce distinctive features, particularly in the energy region of the Coulomb barrier.

In summary, proton-rich radioactive beams by their very nature offer the prospect of unique and distinctive insights into the structure and reaction processes of nuclei in the vicinity of the proton drip-line.

References

Axelsson, L. (and 26 others) 1996 *Phys. Rev.* C **54**, 1511.

Bain, C. R. (and 18 others) 1996 *Phys. Lett.* B **373**, 35.

Beausang, C. W. & Simpson, J. 1996 *J. Phys.* G **22**, 527.

Benenson, W., Guichard, A., Kashy, E., Mueller, D., Nann, H. & Robinson, L. W. 1975 *Phys. Lett.* B **58**, 46.

Blank, B. (and 17 others) 1995 *Phys. Rev. Lett.* **74**, 4611.

Bonche, P., Flocard, H., Heener, P. H., Krieger, S. J. & Weiss, M. S. 1985 *Nucl. Phys.* A **443**, 39.

Borge, M. G. (and 10 others) 1993 *Phys. Lett.* B **317**, 25.

Cameron, J. A., Bentley, M. A., Bruce, A. M., Cunningham, R. A., Gelletly, W., Price, H. G., Simpson, J., Warner, D. D. & James, A. N. 1990 *Phys. Lett.* B **235**, 239.

Cameron, J. A., Bentley, M. A., Bruce, A. M., Cunningham, R. A., Gelletly, W., Price, H. G., Simpson, J., Warner, D. D. & James, A. N. 1991 *Phys. Rev.* C **44**, 1882.

Catford, W. N. (and 26 others) 1996 *Nucl. Inst. Meth. Phys. Res.* A **371**, 449.

Chandler, C. (and 21 others) 1997 *Phys. Rev.* C **56**, R2924.

Chartier, M. (and 16 others) 1996 *Phys. Rev. Lett.* **77**, 2400.

Comay, E., Kelson, I. & Zidon, I. 1988 *Phys. Lett.* B **210**, 31.

Coszach, R. (and 22 others) 1995 *Phys. Lett.* B **353**, 184.

Darquennes, P. (and 18 others) 1990 *Phys. Rev.* C **42**, R804.

D'Auria, J. M., Carraz, L. C., Hansen, P. G., Jonson, B., Mattson, S., Rawn, H. L., Skarestad, M. & Westgaard, L. 1977 *Phys. Lett.* B **66**, 233.

Davids, C. N., Back, B. B., Bindra, K., Henderson, D. J., Kutschera, W., Lauriston, T., Nagane, Y., Singathorn, P., Ramaya, A. V. & Walters, W. B. 1992 *Nucl. Instrum. Meth. Phys. Res.* B **70**, 358.

Davids, C. N. (and 17 others) 1997 *Phys. Rev.* C **55**, 2255.

Davids, C. N. (and 11 others) 1998 *Phys. Rev. Lett.* **80**, 1849.

De Angelis, G., *et al*. 1998 *Phys. Lett.* B. (In the press.)

Ennis, P. J., Lister, C. J., Gelletly, W., Price, H. G., Varley, X., Butler, P. A., Hoare, T., Cwiok, S. & Nazarewicz, W. 1991 *Nucl. Phys.* A **535**, 392.

Gelletly, W. 1995 *Acta Phys. Pol.* B **26**, 323.

Gelletly, W., Bentley, M. A., Price, H. G., Simpson, J., Gross, C., Dushl, J. L., Varley, B. J., Skeppstedt, O. & Rastikerdor, S. 1991 *Phys. Lett.* B **253**, 287.

Görres, J., Wiescler, M. & Thiebemann, F. K. 1995 *Phys. Rev.* C **51**, 392.

Gorska, M. (and 27 others) 1997 *Phys. Rev. Lett.* **79**, 2415.

Grodzins, L. 1966 *Phys. Lett.* **2**, 88.

Hamamoto, I. & Sagawa, H. 1993 *Phys. Rev.* C **48**, R960.

Hansen, P. G. & Jonson, B. 1987 *Europhys. Lett.* **4**, 409.

Hardy, J. C., Towner, I. S., Koslowsky, V. T., Hogberg, E. & Schmeing, H. 1990 *Nucl. Phys.* A **509**, 429.

Heese, J., Blumenthal, D. J., Chishti, A. A., Chaudury, P., Crowell, B., Ennis, P. J., Lister, C. J. & Winter, C. L. 1991 *Phys. Rev.* C **43**, R921.

Helariutta, K. (and 18 others) 1996 *Phys. Rev.* C **54**, R2799.

Holt, R. J. (and 11 others) 1977 *Phys. Lett.* B **69**, 55.

Honkanen, A. *et al*. 1996 University of Jyvasykla preprint 15a/1996.

James, A. N., Morrison, T. P., Ying, K. L., Connell, K. A., Price, H. G. & Simpson, J. 1988 *Nucl. Instrum. Meth. Phys. Res.* A **267**, 144.

Kekelis, G. J., Zisman, M. S., Scott, D. K., John, R., Vineira, D. J., Cerny, J. & Ajzarberg-Selove, F. 1978 *Phys. Rev.* C **17**, 1429.

Koboyashi, T., Yamakawa, O., Omata, K., Sagimoto, K. & Shimoda, T. 1989 *Phys. Rev. Lett.* **60**, 2599.

Kryger, R. A. (and 16 others) 1995 *Phys. Rev. Lett.* **74**, 861.

Lewitowicz, M. (and 28 others) 1994 *Phys. Lett.* B **322**, 20.

Lievens, P., Vermeeven, L., Sliverans, R. E., Arnold, E., Neugant, R., Wendt, K. & Buslinger, F. 1992 *Phys. Rev.* C **46**, 797.

Lister, C. J. (and 13 others) 1985 *Phys. Rev. Lett.* **55**, 810.

Lister, C. J., Ennis, P. J., Chishti, A. A., Varley, B. J., Gelletly, W., Price, H. G. & James, A. N. 1990 *Phys. Rev.* C **42**, R1191.

Möller, P., Nix, J. R. & Kratz, K.-L. 1997 *At. Data Nucl. Data Tables* **66**, 131.

Mueller, A. C. & Anne, R. 1991 *Nucl. Instrum. Meth. Phys. Res.* B **56/57**, 559.

Münzenberg, G., Faust, W., Hofmann, S., Ambruster, P., Güttner, K. & Ewald, H. 1979 *Nucl. Instrum. Meth. Phys. Res.* **161**, 65.

Myers, W. D. 1990 In *Proc. 1st Int. Conf. Radioactive Beams, Berkeley, CA, October 1989* (ed. W. D. Myers, J. M. Nitschke & E. B. Norman), p. 269. World Scientific.

Nagarajan, M. A. *et al*. 1996 Ganil P 95 02.

Nazarewicz, W., Dudek, J., Bengtsson, R., Bengtsson, T. & Ragnarsson, I. 1985 *Nucl. Phys.* A **435**, 397.

O'Leary, C., Bentley, M. A., Appleka, D. E., Cullen, D. M., Erturk, S., Bork, R. A., Maj, A. & Saitoh, T. 1997 *Phys. Rev. Lett.* **79**, 4349.

Oinonen, M. *et al*. 1998 *Phys. Rev.* C. (In the press.)

Onderwater, C. J. G. (and 29 others) 1997 *Phys. Rev. Lett.* **78**, 4893.

Ozawa, A. (and 10 others) 1994 *Phys. Lett.* B **534**, 18.
Paul, E. S. (and 20 others) 1995 *Phys. Rev.* C **51**, 78.
Petrovichi, A., Faessler, A. & Koppel, Th. 1983 *Z. Phys.* A **314**, 227.
Petrovici A., Schmid, K. W. & Foesslor, A. 1996 *Nucl. Phys.* A **605**, 290.
Pfaff, B., Morrisey, D. J., Berenson, W., Farabach, M., Hallström, M., Powell, C. F., Sherrill, B. M., Steiner, M. & Winger, J. A. 1996 *Phys. Rev.* C **53**, 1753.
Raman, S., Nestor, C. W., Kahan, S. & Blott, K. H. 1991 *Phys. Rev.* C **43**, 556.
Regan, P. H. (and 26 others) 1997 *Acta Phys. Pol.* B **28**, 431.
Richter, A. 1993 *Nucl. Phys.* A **553**, 417c.
Rolfs, C. 1973 *Nucl. Phys.* A **217**, 29.
Schmidt, K. (and 10 others) 1994 *Z. Phys.* A **350**, 99.
Schneider, R. (and 13 others) 1994 *Z. Phys.* A **348**, 241.
Schwab, W. (and 16 others) 1995 *Z. Phys.* A **350**, 283.
Sellin, P. J. (and 14 others) 1992 *Nucl. Instrum. Meth. Phys. Res.* A **311**, 217.
Seweryniak, D. (and 20 others) 1998 *Phys. Rev.* C **55**, R2137.
Sherrill, B. M. *et al*. 1991 *Nucl. Instrum. Meth. Phys. Res.* B **56/57**, 1106.
Simon, R. S., Schmidt, K.-H., Hessberger, F. P., Hlawwe, S., Honusek, M., Munzenbera, G., Clare, H. G., Gotherthons, U. & Schwab, W. 1986 *Z. Phys.* A **325**, 197.
Sorlin, O. 1997 In *Proc. Int. Conf. Fission and Properties of Neutron-Rich Nuclei, 10–15 November 1997, Sanibel Island, FL, USA*.
Tanihata, I., Hamagaki, H., Hashimoto, O., Shida, Y., Yashikawa, K., Sagimoto, K., Yamakama, K., Koboyashi, T. & Takah, N. 1985 *Phys. Rev. Lett.* **55**, 2676.
Wallace, R. K. & Woosley, S. E. 1981 *Ap. J. Suppl.* **45**, 389.
Winger, J. A. (and 11 others) 1993 *Phys. Lett.* B **299**, 214.
Woods, P. J. & Davids, C. N. 1997 *A. Rev. Nucl. Part. Sci.* **47**, 541.
Zhukov, M. V. & Thompson, I. J. 1995 *Phys. Rev.* C **52**, 3505.